DOI 10.4430/bgo00451

Automatic fault tracking from 3D seismic data using the 2D Continuous Wavelet Transform combined with a Convolutional Neural Network

S.-A. Ouadfeul[1] and L. Aliouane[2]

[1] *Algerian Petroleum Institute, Sonatrach, Boumerdes, Algeria*
[2] *Earth Physics Laboratory, Faculty of Hydrocarbon and Chemistry, University M"Hamed Bougara, Boumerdes, Algeria*

(Received: 20 July 2023; accepted: 21 January 2024; published online: 29 March 2024)

ABSTRACT The aim of this work is to propose a new technique for automatic fault tracking from 3D seismic data using the 2D Continuous Wavelet Transform (*CWT*) method combined with artificial intelligence. Time slices of the variance attribute, derived from the 3D seismic data and chosen by the user, are analysed using the 2D *CWT* with the 2D Mexican Hat as an analysing wavelet, and the maxima of the modulus of the 2D *CWT* are mapped for the full range of scales. The ensemble of mapped maxima for the set of time slices is filtered using a Convolutional Neural Network machine. Machine training is performed with a supervised mode using the manually tracked faults as a desired output. Application to real data shows the efficiency and robustness of the proposed method, which can greatly help seismic interpreters in avoiding manual fault tracking, a difficult and time-consuming task.

Key words: seismic cube, variance attribute, time slices, 2D *CWT*, CNN, fault tracking.

1. Introduction

Manual fault tracking from 3D seismic data is a difficult and time-consuming task. One of the challenges is signal distortion in the fault neighbourhood and vertical and lateral resolution controlled by high frequency attenuation of the seismic signal in deep geological targets. Many authors have suggested automatic fault tracking approaches. Noori *et al*. (2019) have proposed an approach of automatic fault detection in seismic data based on the Gaussian process regression: they considered geological layers as smooth normal events in seismic sections. Therefore, the location of the fault plane coincides with where the Gaussian process receives an error when describing the layers. Discontinuities, such as faults, cause the Gaussian process to suffer errors near the anomaly. These errors were used and analysed to detect the probable locations of fault edges. Ultimately, a consistent connection algorithm was utilised to separate the most probable fault points and connect them to an edge by means of a morphological reconstruction algorithm. Yu *et al*. (2021) have used the deep Convolutional Neural Network (CNN) for automatic fault tracking from 3D seismic data sets. The authors of the present paper, instead, used an open-source multi-gigabyte expert-labelled field data set in response to the challenge of accessing large-scale expert-labelled field data sets and showed that 2D fault recognition, within this data set, is an image segmentation, or edge detection, problem in the computer vision field, that can be expressed as a pixel-level fault/non-fault binary classification. Guo *et al*. (2020)

have published a paper on fault and horizon tracking using the CNN, with a case study from coalfield, located in the Shanxi province, in China. In our paper, the CNN is combined with the bi-dimensional Continuous Wavelet Transform (*CWT*) to achieve automatic fault tracking from 3D seismic data. It also includes a brief description of the 2D *CWT* and CNN, followed by that of the processing algorithm. Next, an application of the seismic data from the Gulf of Mexico is shown. The interpretation of the results obtained and the conclusions by the authors complete the work.

2. 2D *CWT*

The 2D wavelet decomposition of a given function, $f \in L^2(R^2)$, with an analysing wavelet, $\varnothing \in L^2(R^2)$, is defined for all $a > 0$, $b \in R^2$, by (Grossman and Morlet, 1985; Ouadfeul *et al.*, 2012, 2013):

$$CWT(b_x, b_y, a) = \iint_{R^2} f(x,y)\emptyset^*\left(\frac{x-b_x}{a}, \frac{y-b_y}{a}\right)dxdy \quad (1)$$

where: $\varnothing^*$ denotes the conjugate.

The analysing wavelet must check the admissibility condition (Eq. 2) and must have *N* vanishing moments (Eq. 3) (Grossman and Morlet, 1985):

$$\iint_{R^2} \emptyset(x,y)dxdy = 0 \quad (2)$$

$$\iint_{R^2} P_{N,N}\,\emptyset(x,y)dxdy = 0 \quad (3)$$

where $P_{N,N}$ is a polynomial in $L^2(R^2)$, with *(N, N*) degree:

$$P_{N,N} = \sum_{i=0}^{N}\sum_{j=0}^{N} \alpha_{i,j}\,(xy)^{ij}. \quad (4)$$

Two analysing wavelets, generally used in image processing, are the Gaussian (Eq. 4) and the Mexican Hat (Eq. 5). In this paper, the Mexican Hat is used:

$$\emptyset(x,y) = e^{-0.5(x^2+y^2)} \quad (5)$$

$$\emptyset(x,y) = (2 - x^2 - y^2)e^{-0.5(x^2+y^2)}. \quad (6)$$

The digital representation of Eq. 1 is:

$$CWT(b_{xi}, b_{yj}, a_k) = \sum_{i=1}^{N}\sum_{j=1}^{M} f(x_i, y_j)\emptyset^*\left(\frac{x_i - b_{xi}}{a_k}, \frac{y_j - b_{yj}}{a_k}\right). \quad (7)$$

If $f(x_i, y_j)$ is represented as a matrix $A(i, j)$ of size $N \times M$, the digital form of the 2D *CWT* can be expressed as:

$$CWT(b_{xi}, b_{yj}, a_k) = \sum_{i=1}^{N} \sum_{j=1}^{M} A(i,j)\, \emptyset^*\left(\frac{x_i - b_{xi}}{a_k}, \frac{y_j - b_{yj}}{a_k}\right). \quad (8)$$

The scaling is a power law given by (Ouadfeul and Aliouane, 2013):

$$a_k = a_0 * 2^{k*dk} k = 0{,}1 \ldots\ldots\ldots, L \quad (9)$$

$$a_0 = 2 * \sqrt{dx^2 + dy^2} \quad (10)$$

where *L* is an integer defined by (Ouadfeul and Aliouane, 2013):

$$L = \frac{1}{2 * d_k} \log\left(\frac{(\Delta x * N)^2 + (\Delta y * M)^2}{a_0}\right) / \log(2) \quad (11)$$

where d_k is a real number.

3. The CNN

CNNs are distinguished from other neural networks by their high performance in image and speech processing. These networks comprise three main types of layers, namely:

- the convolutional layer,
- the pooling layer,
- the fully connected layer (FC).

Fig. 1 shows a typical CNN suitable for image classification. The convolutional layer is the first layer of a CNN. While convolutional layers can be followed by additional convolutional layers or pooling layers, the FC is the last layer. For each layer, the CNNs increase in complexity and identify larger portions of an image. Previous layers focus on simple features, such as colours and edges. As the image data progresses through the layers of the CNN, the CNN begins to recognise larger features or shapes of the object until it finally identifies the intended object. The rectified linear unit (ReLU) applies an activation function to the output of the previous layer; the objective of this layer is to add non-linearity to the network.

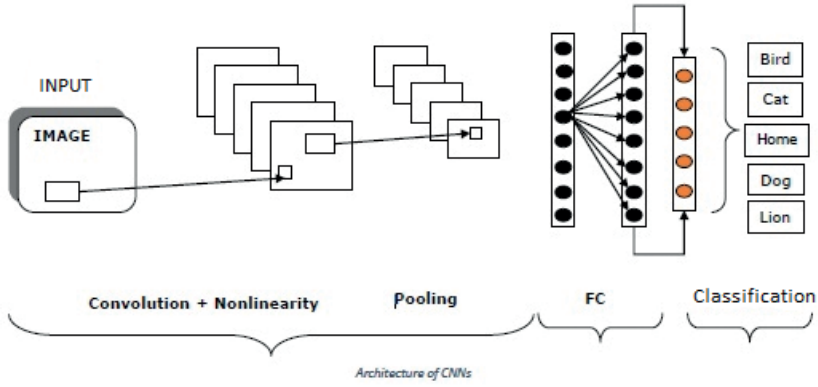

Fig. 1 - The typical architecture of a CNN for image classification.

4. Automatic fault tracking using the 2D *CWT* and CNN

The first step of the proposed approach is to apply the 2D *CWT* to different time slices of the cropped seismic volume using the 2D Mexican Hat as an analysing wavelet. The maxima of the modulus of 2D *CWT* are calculated for each scale using its first and second derivative. The maxima calculated for the full range of scales are plotted in the plan. Random noise and maxima that are not due to faults are, then, filtered from the mapped maxima using a CNN. The goal of this operation is to keep only the maxima that are due to faults. Fig. 2 shows the flow chart of the proposed method.

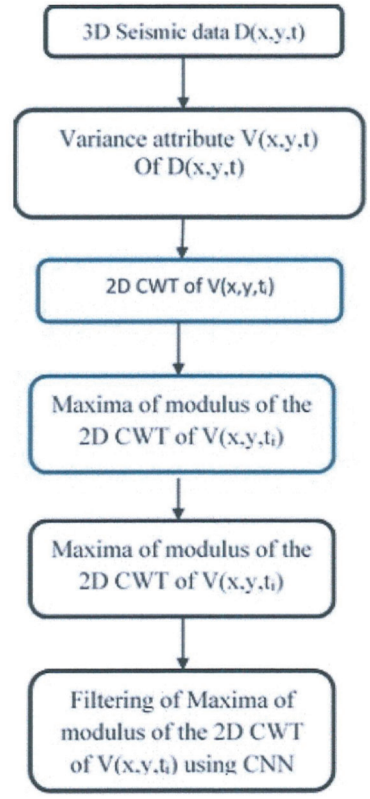

Fig. 2 - Flow chart of fault tracking from 3D seismic data using 2D *CWT* and CNN.

5. Application to real data

To check the efficiency of the proposed data, 3D marine seismic data recorded in the Gulf of Mexico is analysed. In what follows, the analysis of these data, using the 2D continuous wavelet transform, is discussed.

5.1. 3D seismic data analysis using the 2D CWT

The proposed technique is applied to 3D seismic data recorded in the Gulf of Mexico. Fig. 3 shows the 3D seismic cube versus space and time. Fig. 4 shows the cropped volume in the time interval (-1,756, -812 ms). Fig. 5 shows the calculated variance attribute of the cropped

volume with a sliding window that is 3×3×3 in size. The 2D *CWT* of a selection of time slices of the variance attributes is calculated using the 2D Mexican Hat as analysing wavelet, and, then, the maxima of the 2D *CWT* modulus are calculated.

Fig. 6 shows the map of the variance time slice at t = -1752 ms and Fig. 7 shows the modulus of the 2D *CWT* at the smallest scale a = 42 ft. Fig. 8 shows the map of the maxima of the modulus of the 2D *CWT* for the full range of scales, varying from 11.31 to 588.13 ft.

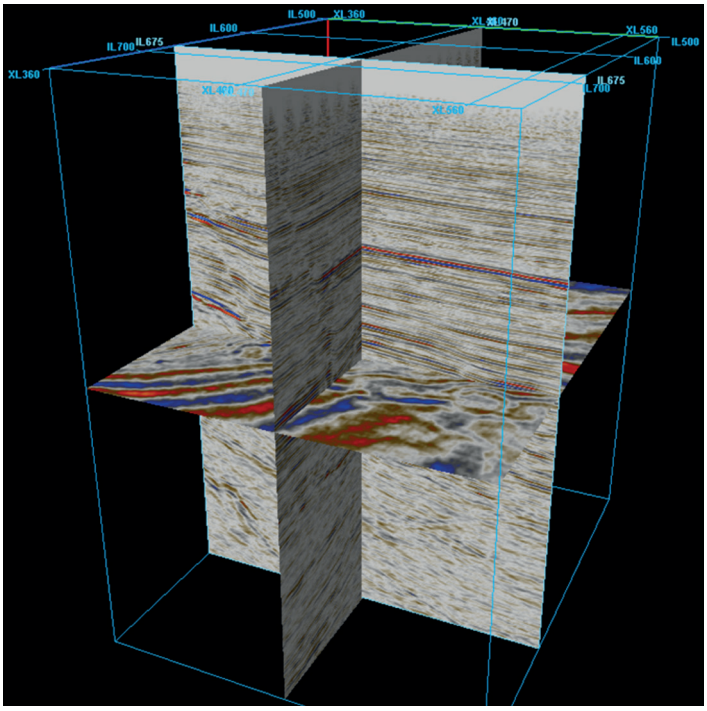

Fig. 3 - 3D seismic cube versus space and time for Inline = 675, Xline = 470, t = -1,752 ms.

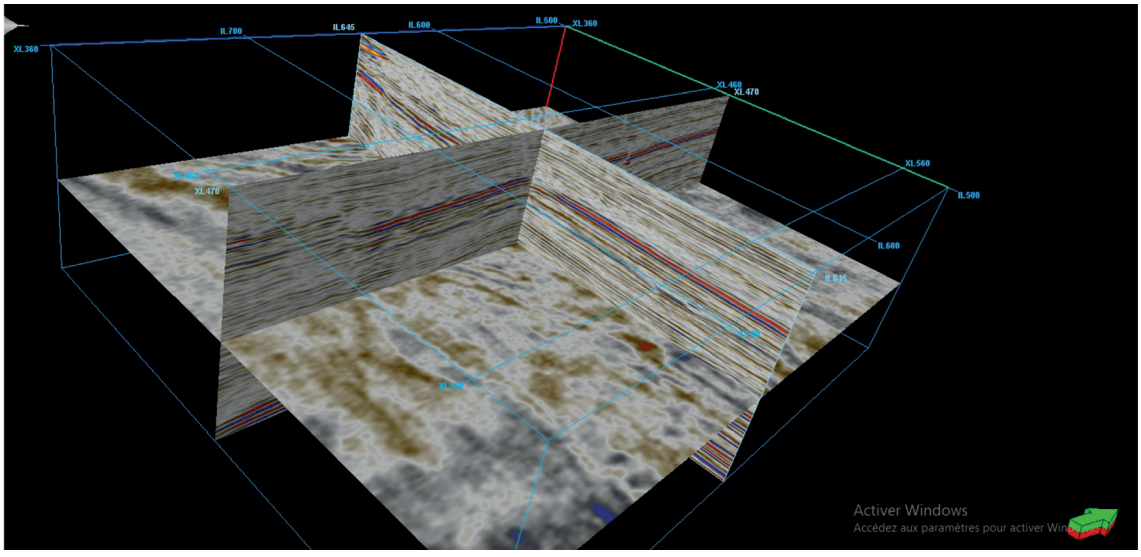

Fig. 4 - Cropped seismic cube versus space and time (Inline = 645, Xline = 470, t = -1,352 ms).

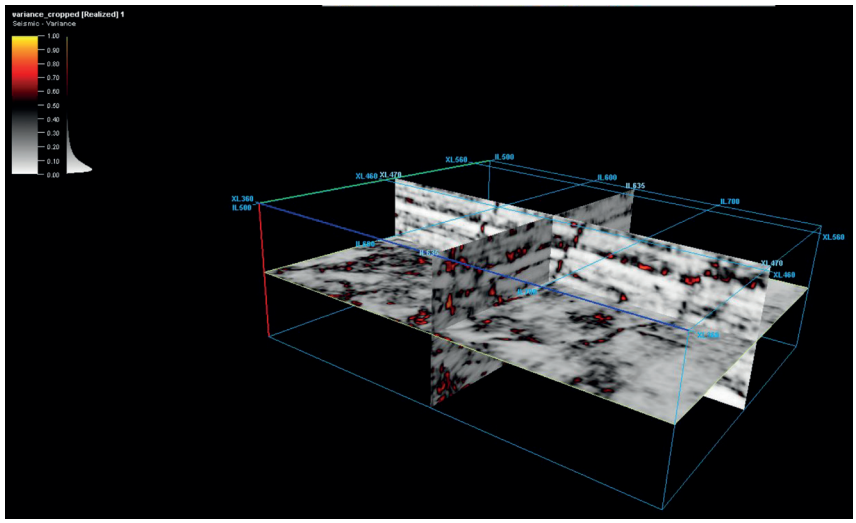

Fig. 5 - Cropped volume of the variance attribute versus space and time (Inline = 635, Xline = 470, t = -1,284 ms).

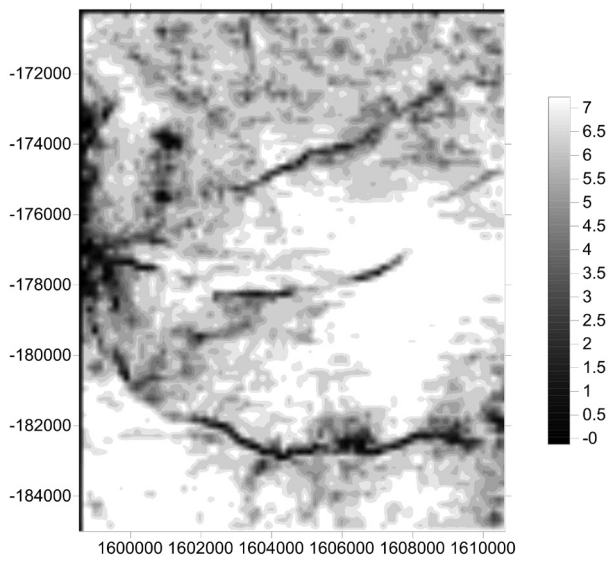

Fig. 6 - Map of a time slice of the variance attribute versus the space at t =-1,752ms.

5.2. Maxima of the modulus of the 2D CWT *analysis using CNN*

The ensemble of the maxima of the modulus of the 2D *CWT* are filtered using a CNN machine, the input is a grey scale image that is 452×760 in size. The filtering operation consists of cleaning edges and keeping only maxima corresponding to faults, since CNN can learn custom edge detection filters based on the probability distribution of pixels in a certain data set and the specific objective of the network. The input data is convolved with a 226×380 median filter, the ReLU operator is applied to data after convolution, followed by maximum pooling. The convolution, ReLU and maximum pooling operators are applied three times; the CNN has only one fully connected layer. These parameters are optimised after many numerical experiences with the faults manually tracked from the raw seismic data shown in Fig. 8 as target.

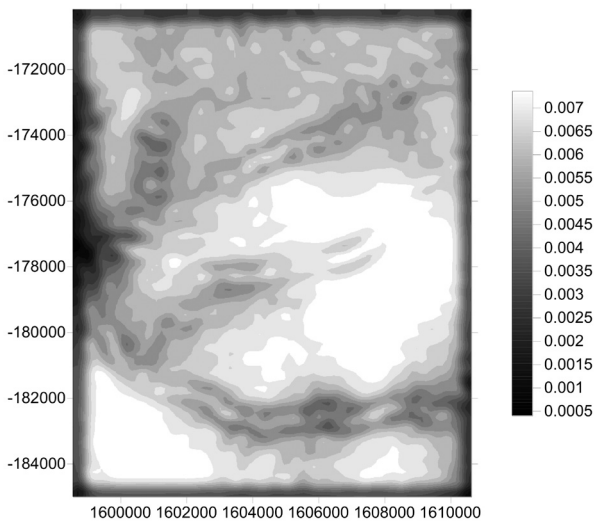

Fig. 7 - Map of the modulus of 2D *CWT* of the time slice shown in Fig. 8 versus the space at the smallest scale a = 11.31 ft.

6. Interpretation of results and conclusions

The whole process is applied to 10 time slices chosen from the cropped seismic cube. Fig. 9 shows the fault network obtained, and the comparison between the faults obtained and those manually tracked demonstrates the possibility of automating the fault tracking operation. To check the efficiency of the proposed method, another CNN machine is implemented to track these faults using the raw seismic data as an input; after 1,000,000 numerical experiences, the weight of connection of this machine is optimised. It is clear that the implemented CNN machine using raw seismic data as an input is very complex and its execution is time consuming compared to the implemented machine using the maxima of the modulus of the 2D *CWT*. To quantitively assess the proposed method, the distances between the faults manually tracked and the faults tracked using the two CNN machines, previously implemented, were measured; the distance between the tracked faults using the raw seismic data as input and the manually tracked faults is 50 times greater than the distance between the tracked faults using the maxima of the modulus of the 2D *CWT* seismic data as input and the manually tracked faults.

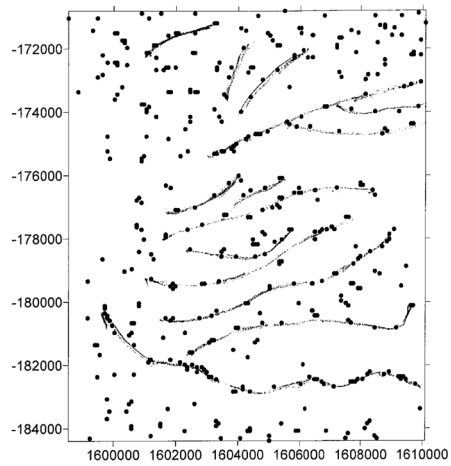

Fig. 8 - Map of the maxima of the modulus of the 2D *CWT* with the tracked faults from raw seismic data blended with the variance attribute.

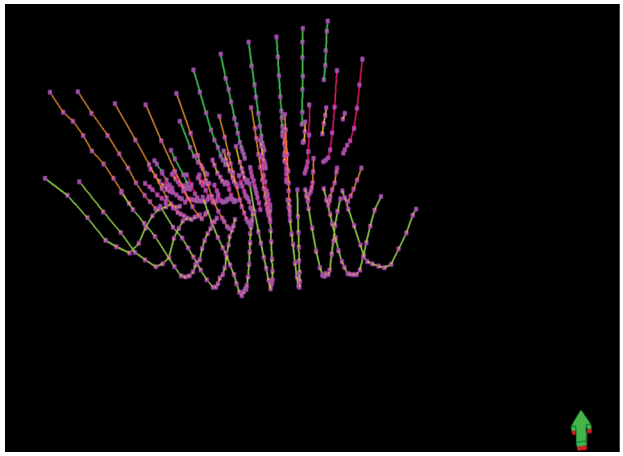

Fig. 9 - The fault network obtained using the 2D *CWT* combined with the CNN.

Automatic fault tracking using a CNN with raw seismic data is very complex and optimisation of the neural machine parameters, such as number of hidden layers and number of neurons in the hidden layers, require a very high number of numerical experiences, which is time consuming and calls for an extremely large amount of computer memory space. The use of the maxima of the modulus of the 2D *CWT*, rather than that of raw seismic data as input of the CNN machine, is able to solve this ambiguity. Consequently, the use of the maxima of modulus maxima lines as an input of CNNs can greatly reduce result uncertainty and solve the complex problem of choosing the CNN parameters, when using raw seismic data as input.

REFERENCES

Grossmann A. and Morlet J.; 1985: *Decompositions of functions into wavelets of constant shape and related transforms.* In: Syreit L. (ed), Mathematics and physics: Lecture on recent results, World Scientific, Singapore City, Singapore, pp. 135-165.

Guo Y., Peng S., Du W. and Li D.; 2020: *Fault and horizon automatic interpretation by CNN: a case study of coalfield.* J. Geophys. Eng., 17, 1016-1025.

Noori M., Hassani H., Javaherian A., Amindavar H. and Torabi S.; 2019: *Automatic fault detection in seismic data using Gaussian process regression.* J. Appl. Geophys., 163, 117-131.

Ouadfeul S.-A. and Aliouane L.; 2013: *Structural edge delimitation from gravity anomaly data using the directional continuous wavelet transform with an example from Basin and the Range province in the United States.* Lead Edge, 32, 1462-1467.

Ouadfeul S.-A., Aliouane L., Hamoudi M., Boudella A. and Eladj S.; 2012: *Multiscale analysis of geophysical signals using the 2D continuous wavelet transform*. In: Baleanu D. (ed), Wavelet Transforms and Their Recent Applications in Biology and Geoscience, InTechOpen, London, UK, pp. 253-276

Ouadfeul S.-A., Hamoudi M., Aliouane L. and Eladj S; 2013: *Aeromagnetic data analysis using the 2D directional continuous wavelet transform (DCWT)*. Arab. J. Geosci., 6, 1669-1680.

Yu A., Guo J., Ye Q., Childs C., Walsh J. and Dong R.; 2021: *Deep convolutional neural network for automatic fault recognition from 3D seismic datasets.* Comput. Geosci., 153, 104776, 12 pp., doi: 10.1016/j.cageo.2021.104776.

Corresponding author: Leila Aliouane
Laboratoire Physique de la Terre
Universite M'Hamed Bougara Boumerdes Faculte des Hydrocarbures et de la Chimie
Boulevard de l'independance, Boumerdes 35000, Algeria
Phone: +213552434986; e-mail: l.aliouane@univ-boumerdes.dz